Published in final edited form as:
J Mol Biol. 2009 March 27; 387(2): 320–334. doi:10.1016/j.jmb.2009.01.059.

CLIC2-RyR1 interaction and structural characterization by cryo-electron microscopy

Xing Meng[1,*], **Guoliang Wang**[2,*], **Cedric Viero**[3,*], **Qiongling Wang**[2], **Wei Mi**[4], **Xiao-Dong Su**[4], **Terence Wagenknecht**[1], **Alan J. Williams**[3,†], **Zheng Liu**[1,†], and **Chang-Cheng Yin**[2,††]

1*Wadsworth Center, New York State Department of Health, Albany, NY 12201, USA*

2*Department of Biophysics, Peking University Health Science Center, Peking University, Beijing 100083, China*

3*Department of Cardiology, Wales Heart Research Institute, Cardiff University School of Medicine, Heath Park, Cardiff CF14 4XN, United Kingdom*

4*National Laboratory of Protein Engineering and Plant Genetic Engineering, College of Life Sciences, Peking University, Beijing 100871, China*

Abstract

Chloride intracellular channel 2 (CLIC2), a newly discovered small protein distantly related to the glutathione transferase (GST) structural family, is highly expressed in cardiac and skeletal muscle although its physiological function in these tissues has not been established. In the present study, [^{3}H]-ryanodine binding, Ca^{2+} efflux from skeletal sarcoplasmic reticulum (SR) vesicles, single channel recording, and cryo-electron microscopy were employed to investigate whether CLIC2 can interact with skeletal ryanodine receptor (RyR1) and modulate its channel activity. We found that: (1) CLIC2 facilitated [^{3}H]-ryanodine binding to skeletal SR and purified RyR1, by increasing the binding affinity of ryanodine for its receptor without significantly changing the apparent maximal binding capacity; (2) CLIC2 reduced the maximal Ca^{2+} efflux rate from skeletal SR vesicles; (3) CLIC2 decreased the open probability of RyR1 channel, through increasing the mean closed time of the channel; (4) CLIC2 bound to a region between domain 5 and domain 6 in the clamp-shaped region of RyR1; (5) and in the same clamp region, domain 9 and domain 10 became separated after CLIC2 binding, indicating CLIC2 induced a conformational change of RyR1. These data suggest that CLIC2 can interact with RyR1 and modulate its channel activity. We propose that CLIC2 functions as an intrinsic stabilizer of the closed state of RyR channels.

Keywords

Ca^{2+}-release channel; Ca^{2+} signaling; Chloride intracellular channel 2; cryo-electron microscopy; ryanodine receptor

†To whom correspondence may be addressed: Alan J. Williams, Ph.D., Department of Cardiology, Wales Heart Research Institute, Cardiff University School of Medicine, Heath Park, Cardiff CF14 4XN, United Kingdom. Tel.: 44-29-20744430; Fax: 44-29-20743500; E-mail: WilliamsAJ9@cardiff.ac.uk; or Zheng Liu, Ph.D., Wadsworth Center, New York State Department of Health, Albany, NY 12201. Tel.: 518-474-6516; Fax: 518-474-7992; Email: liuz@wadsworth.org. ††To whom correspondence should be addressed: Chang-Cheng Yin, Ph.D., Department of Biophysics, Peking University Health Science Center, Peking University, Beijing 100083, China. Tel/Fax: 86-10-82801394; E-mail: ccyin@bjmu.edu.cn.
*These authors contributed equally to this work.

Introduction

The chloride ion is the most abundant anion in the tissues of animals and plants and anion channels in the cells are often referred to as chloride channels. Several classes of chloride channels have been found, of which three are well-characterized: the ligand-gated receptors, the cystic fibrosis transmembrane conductance regulators (CFTR), and the chloride ion channels (CLC).[1] Chloride ion channels are involved in regulation of absorption and secretion of Na^+, setting the cell membrane potential, acidification of cytoplasmic organelles, and regulation of cell volume.[2]

As a new class of chloride channels, chloride intracellular channel (CLIC) proteins, differ from the other classes of chloride ion channels in primary structure and in the transmembrane regions of the tertiary structure.[3] Since the first member of CLIC, p64 (CLIC5), was discovered in bovine kidney, several members of the CLIC family have been found in other tissues from many species, including NCC27 (CLIC1), CLIC2, CLIC3, mtCLIC (CLIC4), and parchorin (CLIC6).[4-11] With the exception of p64 and parchorin, these proteins are composed of ~240 amino acid residues. The CLIC proteins show sequence homology with members of the glutathione S-transferase (GST) superfamily.[12] Another feature of CLIC proteins distinguishable from other ion channels is that they exist in two different forms: either as soluble globular proteins, or as an integral membrane protein that incorporates into lipid bilayers to form ion channels.[7,10,13-19]

Human CLIC2 protein is composed of 247 amino acids and is found in many organs, including the spleen, lung, liver, and in both skeletal and cardiac muscles.[6,20] Consistent with their high degree of primary structure homology, CLIC2 is similar to CLIC1 and CLIC4 in term of tertiary structure.[17,21-23] Like other members of CLIC family, CLIC2 can exist as a soluble globular protein, or incorporate into a lipid bilayer to form a Cl^- channel.[17]

While the membrane-incorporated CLIC2 proteins function as Cl^- channels, the physiological function of the soluble form CLIC proteins is less well defined. Recently, Dulhunty *et al* showed that CLIC2 can interact with the cardiac ryanodine receptor (RyR2) and modulate its calcium release channel activity, implying that CLIC proteins may play a role in the regulation of Ca^{2+} signaling.[20,24] Ryanodine receptors are the major Ca^{2+} release channels in both cardiac and skeletal muscle, they play a crucial role in the Ca^{2+} signaling pathway that govern the muscle excitation-contraction coupling.[25] The gating of RyRs is regulated with a various intracellular messengers, including calmodulin, FK-binding protein, ATP, Ca^{2+}, Mg^{2+}, and protein kinase A.[26] The investigations of Dulhunty *et al* raise several issues: (1) Can CLIC2 also act as a modulator of the skeletal ryanodine receptor channel (RyR1), and as a consequence is CLIC2 a common regulator of both RyR1 and RyR2? (2) Does CLIC2 modulate RyR1 differently from RyR2? (3) How does CLIC2 interact with RyR and regulate its channel activity?

In the present study, we address the above questions by employing several biochemical and electrophysiological approaches, including [^{3}H]-ryanodine binding, Ca^{2+} efflux from skeletal sarcoplasmic reticulum (SR) vesicles, and single channel recording; and ultimately by using the structural approach of three-dimensional cryo-electron microscopy and single particle image processing. Taken together, our results not only provide for the first time a direct evidence for a physical interaction of CLIC2 with RyR1, but they also suggest that the interaction between CLIC2 and RyR1 stabilizes the closed state of the Ca^{2+} release channel.

Results

CLIC2 facilitated [^{3}H]-ryanodine binding to skeletal heavy SR and purified RyR1

Ryanodine is a plant alkaloid, which binds to the open state RyR/Ca^{2+} release channel with high affinity.[27] To test whether CLIC2 can interact with RyR1 and modify its function, we first carried out [^{3}H]-ryanodine binding experiments. As shown in Figure 1A, at a [Ca^{2+}] of 10 μM CLIC2 increased [^{3}H]-ryanodine binding to skeletal heavy SR; binding rose from 1.31 ±0.1 pmol/mg (buffer, n=6) to 1.57±0.03 pmol/mg (15 μM CLIC2, n=6) and then to 1.7±0.01 pmol/mg (30 μM CLIC2, n=6).

To assess whether this effect is due to a direct interaction of CLIC2 with RyR1, we next undertook [^{3}H]-ryanodine binding to purified RyR1. As shown in Figure 1B, CLIC2 increased [^{3}H]-ryanodine binding to purified RyR1, the binding rose from 7.42±0.48 (n=6) to 8.28±1.39 (n=6) pmol/mg at 10 μM [Ca^{2+}], and from 5.01±0.62 (n=6) to 6.90±1.31 (n=6) pmol/mg at 100 μM [Ca^{2+}]. These data demonstrated that CLIC2 can indeed interact with RyR1 and affect [^{3}H]-ryanodine binding to skeletal heavy SR and purified RyR1.

To quantitatively characterize how CLIC2 interacts with RyR1, we did equilibrium saturation experiments and Scatchard analysis. As shown in Figures 1C and 1D, the interaction of CLIC2 with purified RyR1 resulted in an increase in the binding affinity, without significantly changing the apparent maximal binding capacity. In the absence of CLIC2, the dissociation constant K_d for purified RyR1 was 21.92±6.91 nM (n=6). In the presence of 15 μM CLIC2, however, the dissociation constant K_d for purified RyR1 was reduced to 15.00±2.07 nM (n=6). Although the dissociation constant K_d changed significantly, the apparent maximal binding capacity, B_{max}, remained virtually unchanged (62.89±11.96 [control, n=6] *versus* 62.83±4.68 [15 μM CLIC2, n=6] pmol/mg). These data provided evidence that CLIC2 facilitated [^{3}H]-ryanodine binding to skeletal heavy SR and purified RyR1.

In order to more fully describe the interaction between CLIC2 and RyR1, time-dependent association and dissociation experiments were conducted. CLIC2 (15 μM) stimulated the rate of association of [^{3}H]-ryanodine to its receptor (Figure 2A and Table 1). A linear transformation of the association data highlighted this more clearly (Figure 2B). Experiments were also carried out to determine the influence of CLIC2 on the dissociation of bound [^{3}H]-ryanodine from its receptor (Figure 2C and Table 1). Purified RyR1s were labeled with [^{3}H]-ryanodine in the presence of 0, or 15 μM CLIC2, and allowed to equilibrate for 12 h at 24 °C. Aliquots were subsequently diluted 100-fold into a buffer without ryanodine. CLIC2 had no effect on the dissociation of [^{3}H]-ryanodine from its receptor (Figure 2C and Table 1). These data coupled with the CLIC2-dependent increase in the rate of association suggested that the increase in [^{3}H]-ryanodine binding caused by CLIC2 was due solely to an enhancement of the ryanodine association kinetics.

CLIC2 diminished Ca^{2+} efflux from skeletal heavy SR vesicles

The effect of CLIC2 on [^{3}H]-ryanodine binding to skeletal heavy SR vesicles and purified RyR1 is indicative that CLIC2 can interact with RyR1. We then performed experiments of Ca^{2+} efflux from skeletal SR vesicles, to determine whether the interaction between CLIC2 and RyR1 affects the channel activity of RyR1 (Figure 3). After skeletal heavy SR vesicles were partially loaded by addition of four consecutive aliquots of $CaCl_2$, thapsigargin was added to block the SR Ca^{2+}-ATPase/pump, and then Ca^{2+} efflux was monitored. After the blockade of the Ca^{2+}-ATPase/pump, the medium [Ca^{2+}] increased due to Ca^{2+} efflux from heavy SR vesicles, as monitored by the Ca^{2+} indicator antipyrylazo III. The rise in extravesicular [Ca^{2+}] was stopped by ruthenium red, a RyR channel blocker, indicating that Ca^{2+} efflux occurred through the RyR1 channel. The presence of CLIC2 diminished Ca^{2+} efflux, as

indicated by the reduced rate of rise of the curve. The maximal Ca^{2+} efflux rate decreased from 57.08±7.77 nmol/min/mg (control, n=11) to 42.58 ± 5.37 nmol/min/mg (30 μM CLIC2, n=6). These data showed that CLIC2 is an inhibitor of Ca^{2+} efflux from skeletal heavy SR vesicles.

Single channel recordings revealed that CLIC2 stabilized the closed state of the RyR1 channel

To confirm that the inhibitory effect of CLIC2 on Ca^{2+} efflux from heavy SR vesicles is indeed due to a direct interaction of CLIC2 with RyR1 and to characterize the effect of CLIC2 on the RyR1 channel activity, we assessed the effect of CLIC2 on the gating properties of single RyR1 channels incorporated into planar lipid bilayers. To minimize variability in open probability (P_o), single channel recordings were performed in the presence of EMD 41000, a derivative of caffeine that acted as a RyR channel stimulator.[28] As shown in Figure 4, EMD 41000 raised P_o to 0.55±0.13 (n=8 channels), 0.55±0.13 (n=6 channels), and 0.51±0.10 (n=11 channels), when the holding potential was +20 mV, +30 mV and +40 mV, respectively (Figure 4, A-C, upper traces). CLIC2 (7 μM) drastically reduced P_o by 70%, 70%, and 72% at +20 mV, +30 mV and +40 mV, respectively (Figure 4, A-C, lower traces). Statistical analysis indicated that CLIC2 decreased P_o by prolonging the mean close time T_c (increased by a factor of 9, 15, and 30 at +20 mV, +30 mV, and +40 mV, respectively), without significantly affecting the mean open time T_o (Figure 5). It is noteworthy that CLIC2 did not change the conductance of the RyR1 channel since the current-voltage relationship was not modified (data not shown). Furthermore, we observed neither sub-conductance openings nor coupled gating between RyR1 channels in the presence of CLIC2, whereas CLIC2 had previously been shown to induce sub-state activity of the RyR2 channel, and coupled gating between RyR2 channels.[24] These data indicated that CLIC2 is an inhibitor of RyR1 channel opening and that the reduced Ca^{2+} efflux from skeletal heavy SR vesicles observed in the presence of CLIC2 is likely to be a direct consequence of this inhibition; the inhibitory effect of CLIC2 on the RyR channel may be isoform-dependent given that it seems to have somewhat different effects on RyR1 and RyR2.

Cryo-electron microscopy and three-dimensional reconstructions of RyR1+CLIC2 complex

Our [^{3}H]-ryanodine binding, Ca^{2+} efflux, and single channel recording experiments showed that CLIC2 could indeed interact with RyR1 and modify its channel activity. To better assess how CLIC2 causes these effects, we studied the three-dimensional structure of the RyR1 +CLIC2 complex by cryo-electron microscopy and image reconstruction. Figure 6 shows a typical electron micrograph of frozen-hydrated RyR1+CLIC2 complexes. The particle images displayed characteristic RyR1 appearances, with multiple orientations similar to those previously observed for the un-complexed RyR1.[29-31]

Figure 7 shows two-dimensional averages of RyR1+CLIC2 complexes (panel A) and RyR1 molecules (panel B), computed using images of selected particles, which were lying with their 4-fold symmetry axes oriented perpendicular to the carbon support film. These images were aligned by cross-correlation methods. By visual inspection, the averaged images of RyR1 and RyR1+CLIC2 complex appear very similar to each other, and to the two-dimensional averages determined previously for RyR1.[29] Subtraction of the two-dimensional average of RyR1 from that of the RyR1+CLIC2 complex provides a difference map (panel C) that should resolve the position of bound CLIC2, and that perhaps should reveal conformational differences between the two averaged projection structures. In panel C, the brightest white areas, corresponding to the most significant positive densities, representing protein mass present in the RyR1+CLIC2 complex but absent from RyR1. These areas (one of which is highlighted by a circle in Figures 7A, B and C) are located in a region between domain 5 and domain 6 (see the three-dimensional reconstruction in panel D), part of an assemblage of domains that form the corners of the square-shaped cytoplasmic assembly and that have been termed the “clamp”.[32] A statistical analysis

of the difference between the two averaged images indicated that these areas show significant differences at a confidence level greater than 99.9%.[33] These differences almost certainly correspond to the additional mass contributed by bound CLIC2 in the RyR1+CLIC2 complex. This interpretation was confirmed, and the site of difference was mapped more precisely in the three-dimensional reconstructions.

Before computing the three-dimensional reconstruction of the RyR1+CLIC2 complex, we had to address a problem of heterogeneity of the dataset, which caused by partial occupancy of the four CLIC2 binding sites on one RyR1 homo-tetramer. Since the binding affinity between CLIC2 and purified RyR1 is in μM range, we estimate that, under the conditions used for cryo-EM, ~90% of CLIC2 binding sites on RyR1 should be occupied. However, this estimate is for optimal binding conditions, and the actual binding on the EM grids is likely to be lower. For RyR1, the case is even more complicated, because each RyR1 tetramer has four CLIC2 binding sites. Besides the RyR1 molecules showing full occupancy by bound with 4 CLIC2 molecules, there are five other categories of RyR1 molecules that show less than the full complement of four bound CLIC2 molecules (i.e. with 0, 1, 2, or 3 natrin molecules. To estimate the actual percentages of RyR1 with the various complements of bound CLIC2 molecules, we performed a 2D classification analysis. Top images of RyR1+CLIC2 complexes (N=789) were subjected to a multi-reference supervised classification,[34] and the result showed that ~70% of the particles had four CLIC2 molecules bound. The classification allowed us to eliminate most of the incompletely occupied RyR1 particles in the subsequence image processing. We only used the particles with CLIC2 binding sites fully occupied to compute the final 3D reconstruction of RyR1+CLIC2 complex.

In Figure 8A and 8B, the 3D reconstructions of RyR1 and the RyR1+CLIC2 complex are displayed in surface representation, in three orientations. Both reconstructed structures consist of two major components: a large cytoplasmic assembly composed of at least ten distinct domains (labeled by numerals 1–10)[29] and a smaller transmembrane assembly. For the reconstruction of the RyR1+CLIC2 complex, the final resolution was estimated to be 25Å (see Materials and methods). The difference map was masked by simply increasing the threshold of the 3D volume. The density threshold for the 3D volume of control RyR1 is 4.2×10^{-4}, in which the volume of the 3D reconstruction is matched the molecular weight of a tetramer RyR, 2.26 MDa. The density threshold for the 3D volume of RyR1+CLIC2 complex is 4.1×10^{-4}, in which the 3D volume matches the molecular weight 2.37 MDa, a tetramer RyR1 plus 4 CLIC2 molecules. Overall, the 3D reconstruction of RyR1+CLIC2 is very similar to that of RyR1, but close examination reveals some subtle differences. The most noticeable difference was found between domain 5 and domain 6, within the clamp-shaped structures that form each of the corners of the square-shaped cytoplasmic assembly of RyR1.[29] Specifically, the mass between domain 5 and domain 6 of the RyR1+CLIC2 complex appears to be larger than the mass in the corresponding region of the control RyR1 structure. These differences could directly result from the CLIC2 binding, and/or from conformational changes of RyR1 caused by CLIC2 binding. To determine the differences more precisely, we generated a 3D difference map, by subtracting the 3D volume of RyR1 from that of the RyR1+CLIC2 complex. The difference regions were displayed in orange and superimposed on the 3D reconstruction of RyR1 (Figure 8C). The density threshold for the 3D difference map is also 4.1×10^{-4}, identical to the threshold for the RyR1+CLIC2 complex. At a lower density threshold, there are other minor difference showed up, however, it also bring the CLIC2 volume oversized. We simply masked the difference map by increasing the threshold that matches to the RyR1+CLIC2 complex, at this threshold, no other difference was presented. The difference map clearly showed four significant difference features, one associated with each of the copies in the region between domain 5 and domain 6 in the cytoplasmic assembly. RyR1 is a homotetramer composed of four identical monomers, and one CLIC2 molecule binds to each RyR1 monomer, the difference would thus be expected to repeat four times in the 3D difference map. We are

confident that the four significant difference features are directly attributable to the excess mass contributed by the CLIC2 binding to RyR1, because they are the most significant differences that appear when the 3D difference map is displayed at a density threshold value almost the same as the level that was used to image the RyR1+CLIC2 complex and RyR1 structures.

Apart from this area of extra mass between domain 5 and domain 6, the other notable difference is that the linkage between domain 9 and domain 10 in RyR1 has broken in the RyR1+CLIC2 complex (Figure 8B). Domain 9 and domain 10 are also located in the clamp-shaped region of RyR1. The separation between domain 9 and domain 10 is interpreted as a conformational change in RyR1 itself caused by the binding of CLIC2. A similar feature has previously observed in the open state RyR1.[35,36] To further clarify this minor difference, we computed a reverse difference map by subtracting the 3D volume of RyR1+CLIC2 complex from RyR1 control, and display the volume in another color (in blue violet in Figure 8C).

Other minor differences between the two structures can be regarded as insignificant, both in mass and density, and are unlikely to relate specifically to the binding of CLIC2. Reassuringly, the locations of the four major binding sites of CLIC2 on the 3D reconstruction are consistent with the major differences seen in the 2D analysis (Figure 7).

Docking the crystal structure of CLIC2 into the cryo-EM density map

Recently, the crystal structure of CLIC2 has been solved by two research groups.[17,23] We have used one of the atomic structures of CLIC2 to perform an interactive docking by fitting the atomic coordinates (PDB code: 2PER) into the cryo-EM surface envelope of the difference map between RyR1+CLIC2 and RyR1 control. Figure 9 illustrates the fitting of CLIC2, in a view in which the cytoplasmic side of RyR1+CLIC2 complex is tilted from the four-fold symmetry axis. We found that this orientation of the crystal structure of CLIC2 fitted quite well into the cryo-EM density that was assigned to the CLIC2 molecule, as assessed by the cross correlation coefficient values (0.67) between the difference map and the fitted atomic coordinates. Other docking orientations, for example, a 180 degree rotation around the vertical axis (switch the N-terminal domain and foot loop) or 180 degree rotation around the horizontal axis (switch the N-terminal and C-terminal domains), gave lower cross correlation coefficient values.[37] Our docking result clearly illustrates that CLIC2 likely interacts directly with domain 5 and domain 6 of RyR1, with the foot loop interacting with domain 5, and the N-terminal domain and the joint loop region interacting with domain 6.

Discussion

CLIC proteins are found in both skeletal and cardiac muscle of humans and other vertebrates.[6,20] A feature of CLIC proteins that is distinctive from other chloride channels is that they exist in two different forms: soluble and membrane-bound. While the membrane-bound CLIC proteins function as Cl^- channels, the function of soluble CLIC proteins is unknown. Recently, Dulhunty *et al* showed that CLIC2 could interact with RyR2 and modulate its channel activity, demonstrating that CLIC2 is a RyR2 channel regulator, and implying that CLIC proteins may play a role in the regulation of Ca^{2+} signaling.[20,24] Since CLIC2 exists in both cardiac and skeletal muscle and RyR2 shares high homology with RyR1, we speculate that CLIC2 may also interact with and modulate the channel activity of RyR1.

In this report, we investigated the interaction of CLIC2 with the skeletal RyR/Ca^{2+} release channel. We have shown the following: (1) CLIC2 increases [^{3}H]-ryanodine binding to skeletal heavy SR and purified RyR1; (2) CLIC2, in equilibrium saturation [^{3}H]-ryanodine binding experiments, increases the binding affinity of ryanodine for its receptor (i.e., it decreased K_d) without significantly changing the maximal binding capacity (B_{max}); (3) CLIC2 reduces the maximal Ca^{2+} efflux rate from skeletal heavy SR vesicles; (4) CLIC2 decreases the open

probability of RyR1, through increasing the mean closed time of the channel; (5) 3D cryo-electron microscopy of RyR1+CLIC2 complex shows that CLIC2 binds to a region between domain 5 and domain 6 in the clamp-shaped, cytoplasmic regions of RyR1; (6) and the interaction between domains 9 and 10 in the clamp-shaped regions of RyR1 appears to be absent or reduced when CLIC2 binds to RyR1 under conditions that should favor the closed state of RyR1, indicating that CLIC2 induces conformational changes of RyR1 that are distal to its binding site. Our data indicate that CLIC2 can interact with RyR1 and modulate its channel activity.

As CLIC2 has previously been shown to interact with RyR2 this protein may therefore be a common modulator of Ca^{2+} release channels in both cardiac and skeletal muscle.

Effect of CLIC2 on the structure of RyR1

By using cryo-electron microscopy and image reconstruction, we determined the binding site of CLIC2 on RyR1 as being located in an area between domain 5 and domain 6 in the clamp-shaped region of RyR1. Previous studies have shown that the region around domain 5 and domain 6 contains “hotspots” of RyRs, which play important roles in the regulation of these channels. Many critical residues, such as divergent region 2,[38] phosphorylation site S2808,[39] the central disease-causing mutation region,[40] and one proposed coupling site with DHPR,[41] are located in this region. It is not surprising that the binding of CLIC2 to this region could affect the function of RyR1. Intriguingly, domains 5 and domain 6 in RyR1, with which CLIC2 directly interacts, contain the two mutation hotspots that we have previously mapped, the N-terminal disease-causing mutation region and the central disease-causing mutation region.[40,42] Over one hundred mutations in the RyR1 have been identified in families with malignant hyperthermia and central core disease, and these mutations are largely clustered into three regions of RyR1’s ~5,000 amino-acid sequence: amino-terminal region (amino acid residues 35-614), central region (1,728-2,728), and carboxyl-terminal region (3,348-4,973).[43] The two mutation hotspots that lie in cytoplasmic region: the N-terminal region and the central region, are well separated in the primary sequence (> 1,100 amino acids). According to a hypothesis proposed by Ikemoto and colleagues,[44] the two mutation hotspots occur in structural domains that physically interact in the three-dimensional structure, and changes in the strength of their interaction affect channel gating. In that hypothesis, the N-terminal domain and central domain interact in such a way as serve as a regulatory switch for channel gating activity; a tight “zipping” of the interacting domains stabilizes the channel in the closed state. A mutation in either domain weakens the domain-domain interaction, thus increasing the tendency toward “unzipping”; such an unzipping causes activation and leakiness of the Ca^{2+} release channel.

Our structural information, together with the domain switch hypothesis, leads us to propose a molecular mechanism for CLIC2’s inhibition of the RyR1 Ca^{2+} release channel. As illustrated in Figure 9B, the N-terminal domain and the joint loop of CLIC2 interact with domain 6, where the central region is located, and the foot loop of CLIC2 interacts with domain 5, where the N-terminal region is located. It is likely that binding of CLIC2 to domain 5 and domain 6 of RyR1 concurrently strengthens the interaction between these two domains, thereby minimizes domain switch unzipping and stabilizes the closed state of the RyR1 channel. Previously, we have shown that Natrin, a toxin protein from the venom of snake *Naja naja atra*, also binds to domain 5 and domain 6 of RyR1 concurrently, and inhibits the channel activity of RyR1.[45] Our structural information suggests that both Natrin toxin and CLIC2 interact with and inhibit RyR1 channel in a similar manner, which conforms to the domain switch mechanism.

Domain 9 and domain 10 in the clamp-shaped region of RyR1 are thought to be involved in the gating of the RyR1 channel.[35,36] It was reported that domains 9 and domain 10 were linked in the closed state of RyR1 and the central channel in the transmembrane domain appeared to

be closed, whereas they were separated in an open state of RyR1 and the central channel appeared open.[36] We observed that domain 9 and domain 10 were separated upon CLIC2 binding to the closed state RyR1, but the central channel appears to be closed (see Figure 8A and 8B).

Effect of CLIC2 on the function of RyR1

As a Ca^{2+} release channel in the skeletal SR, the activity of RyR1 is modulated by many endogenous and exogenous regulators. In general, channel activators such as cytosolic Ca^{2+} (in the micromolar range), ATP and caffeine increase the P_o of the RyR1 channel and enhance [^{3}H]-ryanodine binding; channel inhibitors such as ruthenium red and Mg^{2+} and Ca^{2+} (in the millimolar range) lower RyR1 P_o and reduce [^{3}H]-ryanodine binding to the channel. As a consequence it has become largely accepted that the ryanodine binding site on the RyR channel is only accessible when the channel is in an open conformation. The results presented in this communication demonstrate that CLIC2 is a RyR channel ligand that does not conform to this general pattern. CLIC2 reduces single channel P_o and RyR1-mediated Ca^{2+} efflux from heavy SR but unexpectedly increases the affinity of the receptor for [^{3}H]-ryanodine. Similar, seemingly contradictory, effects were observed when CLIC2 was added to RyR2.[20,24]

The novel cryo-electron microscopy data presented in this study provides information that may contribute towards an understanding of this phenomenon. Previous investigations have defined specific structural rearrangements associated with the transition of the RyR1 channel from a closed to an open conformation; these include separation of domains 9 and 10 in the cytoplasmic clamp region of the channel and the appearance of a central opening in the transmembrane region.[36] The interaction of CLIC2 with the closed RyR1 channel induces a separation of domains 9 and 10 of the molecule but no equivalent changes in the transmembrane region. The cryo-electron microscopy results on RyR1-CLIC2, albeit at too low a resolution to provide a molecular mechanism of CLIC2's effects on RyR1, nevertheless show structural features that have previously been attributed to the open and to the closed forms of the channel[35,36] that might be related to the biochemical/functional assays that showed characteristics of both "open" (in the clamp regions) and "closed" (in the central region of the transmembrane domain) channel states in the RyR1-CLIC2 complex. We suggest that the binding of CLIC2 to the closed RyR1 induces a conformational change that resembles the "open" configuration in the clamp-shaped region of RyR1, which may facilitate the association of ryanodine to the binding site, and consequently increase its [^{3}H]-ryanodine binding affinity. However, the binding of CLIC2 to domain 5 and domain 6 of RyR1 concurrently strengthens the interaction between these two domains, thereby minimizes domain switch unzipping and stabilizes the closed state of the RyR1 channel, and consequently reduces the rate of Ca^{2+} efflux from skeletal heavy SR.

Finally, CLIC2 resembles the effect of FKBP12 on RyR1.[46,47] In the latter work indeed, FKBP12 was shown to decrease P_o after caffeine activation of skeletal RyR channels; in the absence of FKBP12, RyR1 channels exhibit increased gating frequency, suggesting that FKBP12 "stabilizes" the channel in the open and closed states. Our results suggest that CLIC2, in a manner quite similar to FKBP12, may be an intrinsic stabilizer of the RyR1 channel.

FKP12 interacts, as CLIC2 does, with RyR1's clamp regions, but at a distinct site (involving domains 9-10 and 3) from that where CLIC2 interacts (involving domain 5 and 6).[48] The FKBP12 binds to the periphery between domains 3 and 9, whereas the CLIC2 we mapped is located on top of domains 5 and 6. A sequence between residues 216–572 in RyR1 has sequence homology to an IP_3-binding core region, and a homology model was docking inside domain 5.[49] In another report, the N-terminal residues 41–420 of RyR1 was found has high sequence homology to phosphorylated isocitrate dehydrogenase, a homology model was also docking inside domains 5 and 9.[50] Both of these dockings are in close proximity to the mapped CLIC2

binding site, but at distinct sites. These structural studies lends further support to the hypothesis that the clamp regions of RyR are of critical importance to regulating the channel activity of RyR1, even though they are spatially far remote from the actual ion channel. How these rather remote regulatory sites can affect the conformations in the transmembrane domains bringing the channel into more open or closed state, however, require further high-resolution structural work.

Materials and methods

Chemicals

All chemicals were of analytical grade or above and were purchased from Sigma-Aldrich (St. Louis, Missouri, USA) unless otherwise specified.

CLIC2 expression and purification

CLIC2 was expressed and purified according to methods described in the literature.[23] Briefly, CLIC2 was expressed with an N-terminal His6-tag and purified with Ni^{2+}-chelating column and a gel-filtration chromatography. The final buffer in which purified CLIC2 was dissolved was 20 mM Tris-HCl (pH 7.5) and 200 mM NaCl.

Preparation of skeletal heavy SR vesicles

Skeletal heavy SR (heavy SR) vesicles were prepared from New Zealand white rabbit muscle according to methods described in the literature[51] with some modifications. Briefly, skeletal muscle was homogenized in 5 volumes (v/w) of buffer A (0.3 M sucrose, 10 mM Hepes, pH 7.0, 0.5 mM EDTA, 2 mM PMSF and 1:1000 diluted protease inhibitory cocktail (Sigma P8340). Two steps of differential centrifugation were carried out in sequence, 15 min at 11,000g followed by 1 hr at 110,000g. The pellet from the second centrifugation was collected and re-suspended in buffer A with 0.65 M KCl, with a ratio of 1:1 (w/v: weight of skeletal muscle initially used/volume of KCl extraction buffer), and incubated on ice for 1 hr. The suspension was then re-pelleted and re-homogenized, aliquoted, and layered onto a sucrose step gradient. The gradient steps from bottom to top are 45% (w/v), 38%, 32%, and 27% sucrose. After centrifugation for 16 hr in a Beckman SW28 rotor at 20,000 rpm (70,000g), the membrane fraction (heavy SR) at the interface between 38% and 45% sucrose was collected, diluted approximately two-fold with buffer A and centrifuged again for 1 hr at 110,000g. The pellets were re-suspended in buffer A without EDTA and quick-frozen in liquid nitrogen, and stored at −80 °C until required. Protein concentration was measured with the BCA method according to manufacturer's instruction.

RyR1 purification

RyR1 was purified from CHAPS solublized skeletal heavy SR according to methods described in the literature[52-54] with some modifications. Briefly, skeletal heavy SR vesicles (50 mg) were suspended in 20 ml of buffer B (1 M NaCl, 20 mM Hepes, pH 7.0, 2 mM DTT, 2 mM PMSF, 1:1000 diluted protease inhibitory cocktail) and appropriate CHAPS-soybean phospholipids mixture (10% CHAPS and 5% soybean phospholipids, all from Calbiochem, La Jolla, California, USA). The CHAPS/protein weight ratio was 13.3. After incubation on ice for 30 min with shaking, the sample was centrifuged for 1 hr at 110,000g. The supernatant was loaded onto a hydroxyapatite ceramic (Bio-Rad, Hercules, California, USA) column (5 ml) pre-equilibrated with buffer C (10 mM K_2HPO_4, pH 7.0, 0.5% CHAPS, 0.25% soybean lecithin, 2 mM DTT). The column was washed sequentially with 15 ml of buffer C and buffer D (10 mM K_2HPO_4, 200 mM NaCl, pH 7.0, 0.5% CHAPS, 0.25% soybean lecithin, 2 mM DTT) and buffer E (50 mM K_2HPO_4, 200 mM NaCl, pH 7.0, 0.5% CHAPS, 0.25% soybean lecithin, 2 mM DTT). The 15 ml elute was collected and concentrated by centrifugation at

1000g in a Centricon concentrator (MWCF 100kDa; Millipore, Billerica, Massachusetts, USA.) for further purification on a 5% to 20% (w/v) linear sucrose gradient buffered with buffer B and 0.5% CHAPS, 0.25% soybean lecithin. After centrifugation for 16 hr in a Beckman SW28 rotor at 26,000 rpm (110,000g), the gradient was fractionated into 2 ml portions. After checking by SDS-PAGE, the RyR1-containing fractions were pooled and concentrated as described earlier (29), followed by division into 50 μl aliquots, quick-frozen in liquid nitrogen, and stored at −80 °C until required.

[^{3}H]-ryanodine binding assay

[^{3}H]-ryanodine binding experiments were carried out according to methods described in the literature.[24] Skeletal heavy SR vesicles (0.25 mg/ml) or purified RyR1 (25 μg/ml) were incubated with 0.2 M KCl, 20 mM Hepes, pH 7.0, with various concentrations of Ca^{2+} and [^{3}H]-ryanodine (Perkin-Elmer, Waltham, Massachusetts, USA), and with different concentrations of CLIC2 (15 μM or 30 μM) or buffer only without CLIC2, various concentrations of Ca^{2+} and [^{3}H]-ryanodine were present during the incubation period. The binding reaction was stopped by rapid filtration through Whatman GF/B glass fiber filters pre-soaked with 1% polyethyleneimine, which were then rinsed twice with 10 ml of ice-cold buffer containing 0.2 M KCl and 20 mM Hepes, pH 7.0. The filters were air-dried and placed into 20 ml scintillation vials with 5 ml of scintillation solution (2.5 g PPO and 150 mg POPOP in 500 ml dimethyl benzene), incubated overnight, and the radioactivity was counted the following day. Free Ca^{2+} concentrations were calculated using the computer program of Fabiato and Fabiato.[55] Non-specific binding was measured in the presence of a 1000-fold excess of unlabeled ryanodine (Calbiochem, La Jolla, California, USA). The experiments were repeated at least twice on two different skeletal heavy SR preparations and on purified RyR1 preparations. For details of individual experiments, refer to the figure legends.

Measurement of association/dissociation kinetics

[^{3}H]-ryanodine association/dissociation kinetics experiments were carried out according to methods described in the literature.[56] The association rate of [^{3}H]-ryanodine (2 nM) was measured by quenching the binding reaction by filtration at times ranging from 1 to 500 min after the addition of purified RyR1 (25 μg/ml) to the [^{3}H]-ryanodine reaction medium (1 mM $CaCl_2$, 1 mM EGTA, 0.2 M KCl, 20 mM Hepes, 0.5% CHAPS, 0.25% soybean lecithin, pH 7.0). Dissociation of [^{3}H]-ryanodine from the equilibrium complex followed equilibration of [^{3}H]-ryanodine with purified RyR1 in the presence of 0, or 15 μM CLIC2, and allowed to equilibrate for 12 h at 24 °C. Aliquots were subsequently diluted 100-fold into a buffer without ryanodine. Determinations of residual specific binding were made at times ranging from 5 to 600 min.

Ca^{2+} efflux from skeletal heavy SR vesicles

Experiments were carried out according to methods described in the literature.[57] Briefly, skeletal heavy SR vesicles (100 μg/ml) were added to a 2 ml solution containing 100 mM KH_2PO_4 (pH = 7); 4 mM $MgCl_2$; 1 mM Na_2ATP, and 0.5 mM antipyrylazo III. The temperature was maintained at 25 °C. Extra-vesicular [Ca^{2+}] was monitored at 710 nm using a HITACHI U2010 spectrophotometer. Vesicles were loaded with Ca^{2+} by addition of four aliquots of $CaCl_2$, each initially increasing the extra-vesicular [Ca^{2+}] by 7.5 μM. Sufficient time (2-5 min) was allowed between one addition of Ca^{2+} and the next, so that the uptake reduced the Ca^{2+} concentration to baseline level. Thapsigargin (TG, 200 nM,) was added to block the Ca^{2+}-ATPase/pump, and Ca^{2+} efflux was then measured for 10 min. Ruthenium red (5 μM) was added to confirm that Ca^{2+} efflux was through RyR1. Finally, the Ca^{2+} ionophore A23187 (3 μg/ml) was added, to release all the Ca^{2+} remaining in the vesicles. Experiments were performed with buffer containing no CLIC2, or with 30 μM CLIC2, added together with

skeletal heavy SR. A calibration curve was established at the start of each experiment by measuring changes in antipyrylazo III absorption in response to four sequential additions of 7.5 μM $CaCl_2$.

Single channel recordings

Single channel recordings were conducted as described previously.[58] Planar phospholipid bilayers were formed from suspensions of phosphatidylethanolamine (Avanti Polar Lipids, Alabaster, Alabama, USA) in *n*-decane (35 mg/ml) across a 200-μm diameter hole in a polystyrene copolymer partition that separated two chambers referred to as *cis* (0.5 ml) and *trans* (1.0 ml). The *trans* chamber was held at virtual ground, whereas the *cis* chamber could be clamped at holding potentials relative to ground. Current flow across the bilayer was monitored by an operational amplifier as current-voltage converter.[59] Bilayers were formed with solutions containing 600 mM KCl, 20 mM HEPES, titrated to pH 7.2 with KOH, resulting in a solution containing 610 mM K^+ in both chambers. An osmotic gradient was created by the addition of 2 aliquots (100 μl each) of 3 M KCl to the *cis* chamber. Purified RyR1 proteins were added to the *cis* chamber and stirred. Under these conditions, channels usually incorporated into the bilayer within 5 minutes. If channels did not incorporate, a third aliquot of 3 M KCl could be added to the *cis* chamber. After channel incorporation, further fusion was prevented by perfusion of the *cis* chamber with 610 mM K^+. Channel proteins incorporate into the bilayer in a fixed orientation, so that the cytosolic face of the channel is exposed to the solution in the *cis* chamber, and the luminal face of the channel is exposed to the solution in the *trans* chamber. Single channel open probability P_o was increased by the addition to the *cis* chamber of 20 to 100 μM EMD 41000[28] in all experiments, to minimize P_o variability. Experiments were carried out at room temperature (22 °C). CLIC2 was added to the *cis* chamber 5 min before recording.

Single channel current fluctuations were filtered at 1 kHz with a low pass filter, digitized and displayed in the program Acquire 5.0 (Bruxton Corporation, Seattle, Washington, USA). For analysis, filtered data representing 30 to 120 s of channel activity were digitized and replayed. Single channel current amplitudes and lifetimes were measured from digitized data with the software TAC 3.0 (Bruxton Corporation, Seattle, Washington, USA).

Cryo-electron microscopy (cryo-EM) and image processing

For preparation of the sample of RyR1+CLIC2 complex, RyR1 (50 μg/ml) and CLIC2 (9.28 μM) were incubated in buffer (20 mM Na-MOPS, pH7.4, 200 mM NaCl, 2.0 mM EGTA, 0.5% CHAPS, 2 mM DTT, and 2.0 μg/ml leupeptin) for 30 minutes at 4°C. EM grids were prepared for cryo-EM by an FEI Vitrobot computer-controlled freeze-plunging instrument (FEI Company, Hillsboro, Oregon, USA). Micrographs were recorded with low-dose protocols on an FEI Tecnai F20 field emission gun transmission electron microscope operated at 200 kV, equipped with an Oxford CT3500 cryo-transfer holder (Gatan, Inc., Warrendale, Pennsylvania, USA). The temperature of the grids was maintained at around −170 °C. The defocus of the micrographs ranged between -1.5 and -4.5 μm, at a magnification of 50,760× (±2%). The RyRs have a preferred orientation on the carbon support film of the EM grids, and so to obtain an adequate sampling of orientation, we have collected additional EM data with the specimen grids tilted up to 50°. Tilting provides us the additional orientational views of the RyR molecule that are required to compute accurate 3D reconstructions (see Figure S1 in Supplementary Material). Each exposure corresponded to an electron dose of ~10 $e^-/Å^2$. Micrographs were checked for drift, astigmatism, and presence of Thon rings by optical diffraction. Selected electron micrographs were digitized on a Zeiss/Imaging scanner (Z/I Imaging Corporation, Huntsville, Alabama, USA) with a step size of 14 μm.

Images were processed using the SPIDER/WEB software package.[60] The contrast transfer function effect was corrected to each individual particle using the phase flipping method.[61] For tilted images, each micrograph was divided into small pieces (about 1500 pixel × 800 pixel), the defocus value was estimated for each piece using the SPIDER program, and the defocus value for a particular piece was assigned to all particles lying within the piece. The error of defocus values between particles at different locations within one piece of titled micrograph is about 0.1 μm, similar to the error range of the defocus values. 3D reconstructions were obtained from images of particles lying in all available orientations, through a projection matching procedure.[62] The final three-dimensional reconstructions of RyR1 control (un-complexed) and of the RyR1+CLIC2 complex were computed from 16,519 and 15,889 particle images, respectively. Four-fold symmetry was enforced in all 3D reconstructions. The final resolutions were estimated by the Fourier shell correlation with a cut-off of 0.5,[63] for RyR1 control structure, the resolution is 21 Å; and for the RyR1+CLIC2 complex structure, 25Å. An X-ray structure of CLIC2 (PDB code 2PER) was docked into the cryo-EM density of the 3D difference map manually, using the molecular graphics programs O and Chimera. Various possible fitting orientations were evaluated by the correlation coefficient using the SPIDER program, and best fitting orientation was chose by the highest correlation coefficient.[37]

Statistics

Results were analyzed using a Mann-Whitney rank sum test (SigmaStat software, Systat Software Inc., San Jose, California, USA). Furthermore, if a normality test was successful, a t-test was then undertaken. Effects were regarded as significant when $p<0.05$. The results are expressed as mean values ± S.E.M.

Acknowledgements

This work was supported by research grants from Natural Science Foundation of China, Trans-Century Talent Awarding Program, Ministry of Education, and National Basic Research Program (973 Program), Ministry of Science and Technology, P. R. China to CCY, research grants from the British Heart Foundation to AJW, by American Heart Association grant 0430076N to ZL, and by National Institutes of Health grant AR40615 to TW. We thank Bin Geng (Department of Physiology, The Health Science Centre, Peking University) for excellent technical assistance, and the Wadsworth Center's Electron Microscopy Core Facility and the Resource for Visualization of Biological Complexity (NIH Biotechnological Resource Grant RR01219).

References

1. Jentsch TJ. CLC chloride channels and transporters: from genes to protein structure, pathology and physiology. Crit Rev Biochem Mol Biol 2008;43:3–36. [PubMed: 18307107]
2. Strange K, Emma F, Jackson PS. Cellular and molecular physiology of volume-sensitive anion channels. Am J Physiol 1996;270:C711–730. [PubMed: 8638650]
3. Ashley RH. Challenging accepted ion channel biology: p64 and the CLIC family of putative intracellular anion channel proteins. Mol Membr Biol 2003;20:1–11. [PubMed: 12745921]
4. Landry D, Sullivan S, Nicolaides M, Redhead C, Edelman A, Field M, al-Awqati Q, Edwards J. Molecular cloning and characterization of p64, a chloride channel protein from kidney microsomes. J Biol Chem 1993;268:14948–14955. [PubMed: 7686908]
5. Valenzuela SM, Martin DK, Por SB, Robbins JM, Warton K, Bootcov MR, Schofield PR, Campbell TJ, Breit SN. Molecular cloning and expression of a chloride ion channel of cell nuclei. J Biol Chem 1997;272:12575–12582. [PubMed: 9139710]
6. Heiss NS, Poustka A. Genomic structure of a novel chloride channel gene, CLIC2, in Xq28. Genomics 1997;45:224–228. [PubMed: 9339381]
7. Qian Z, Okuhara D, Abe MK, Rosner MR. Molecular cloning and characterization of a mitogen-activated protein kinase-associated intracellular chloride channel. J Biol Chem 1999;274:1621–1627. [PubMed: 9880541]

8. Duncan RR, Westwood PK, Boyd A, Ashley RH. Rat brain p64H1, expression of a new member of the p64 chloride channel protein family in endoplasmic reticulum. J Biol Chem 1997;272:23880–23886. [PubMed: 9295337]
9. Berryman M, Bretscher A. Identification of a novel member of the chloride intracellular channel gene family (CLIC5) that associates with the actin cytoskeleton of placental microvilli. Mol Biol Cell 2000;11:1509–1521. [PubMed: 10793131]
10. Nishizawa T, Nagao T, Iwatsubo T, Forte JG, Urushidani T. Molecular cloning and characterization of a novel chloride intracellular channel-related protein, parchorin, expressed in water-secreting cells. J Biol Chem 2000;275:11164–11173. [PubMed: 10753923]
11. Berry KL, Bulow HE, Hall DH, Hobert O. A C. elegans CLIC-like protein required for intracellular tube formation and maintenance. Science 2003;302:2134–2137. [PubMed: 14684823]
12. Dulhunty A, Gage P, Curtis S, Chelvanayagam G, Board P. The glutathione transferase structural family includes a nuclear chloride channel and a ryanodine receptor calcium release channel modulator. J Biol Chem 2001;276:3319–3323. [PubMed: 11035031]
13. Edwards JC. A novel p64-related Cl-channel: subcellular distribution and nephron segment-specific expression. Am J Physiol 1999;276:F398–408. [PubMed: 10070163]
14. Tulk BM, Schlesinger PH, Kapadia SA, Edwards JC. CLIC-1 functions as a chloride channel when expressed and purified from bacteria. J Biol Chem 2000;275:26986–26993. [PubMed: 10874038]
15. Tulk BM, Kapadia S, Edwards JC. CLIC1 inserts from the aqueous phase into phospholipid membranes, where it functions as an anion channel. Am J Physiol Cell Physiol 2002;282:C1103–1112. [PubMed: 11940526]
16. Littler DR, Harrop SJ, Fairlie WD, Brown LJ, Pankhurst GJ, Pankhurst S, DeMaere MZ, Campbell TJ, Bauskin AR, Tonini R, Mazzanti M, Breit SN, Curmi PMG. The intracellular chloride ion channel protein CLIC1 undergoes a redox-controlled structural transition. J Biol Chem 2004;279:9298–9305. [PubMed: 14613939]
17. Cromer BA, Gorman MA, Hansen G, Adams JJ, Coggan M, Littler DR, Brown LJ, Mazzanti M, Breit SN, Curmi PM, Dulhunty AF, Board PG, Parker MW. Structure of the Janus protein human CLIC2. J Mol Biol 2007;374:719–731. [PubMed: 17945253]
18. Proutski I, Karoulias N, Ashley RH. Overexpressed chloride intracellular channel protein CLIC4 (p64H1) is an essential component of novel plasma membrane anion channels. Biochem Biophys Res Commun 2002;297:317–322. [PubMed: 12237120]
19. Berryman M, Bruno J, Price J, Edwards JC. CLIC-5A functions as a chloride channel in vitro and associates with the cortical actin cytoskeleton in vitro and in vivo. J Biol Chem 2004;279:34794–34801. [PubMed: 15184393]
20. Board PG, Coggan M, Watson S, Gage PW, Dulhunty AF. CLIC-2 modulates cardiac ryanodine receptor Ca^{2+} release channels. Int J Biochem Cell Biol 2004;36:1599–1612. [PubMed: 15147738]
21. Harrop SJ, DeMaere MZ, Fairlie WD, Reztsova T, Valenzuela SM, Mazzanti M, Tonini R, Qiu MR, Jankova L, Warton K, Bauskin AR, Wu WM, Pankhurst S, Campbell TJ, Breit SN, Curmi PM. Crystal structure of a soluble form of the intracellular chloride ion channel CLIC1 (NCC27) at 1.4-Å resolution. J Biol Chem 2001;276:44993–45000. [PubMed: 11551966]
22. Littler DR, Assaad NN, Harrop SJ, Brown LJ, Pankhurst GJ, Luciani P, Aguilar MI, Mazzanti M, Berryman MA, Breit SN, Curmi PMG. Crystal structure of the soluble form of the redox-regulated chloride ion channel protein CLIC4. FEBS J 2005;272:4996–5007. [PubMed: 16176272]
23. Mi W, Liang Y-H, Li L, Su X-D. The crystal structure of human chloride intracellular channel protein 2: a disulfide bond with functional implications. Proteins 2008;71:509–513. [PubMed: 18186468]
24. Dulhunty AF, Pouliquin P, Coggan M, Gage PW, Board PG. A recently identified member of the glutathione transferase structural family modifies cardiac RyR2 substate activity, coupled gating and activation by Ca^{2+} and ATP. Biochem J 2005;390:333–343. [PubMed: 15916532]
25. Fill M, Copello JA. Ryanodine receptor calcium release channels. Physiol Rev 2002;82:893–922. [PubMed: 12270947]
26. Meissner G. Molecular regulation of cardiac ryanodine receptor ion channel. Cell Calcium 2004;35:621–628. [PubMed: 15110152]
27. Meissner G, el-Hashem A. Ryanodine as a functional probe of the skeletal muscle sarcoplasmic reticulum Ca^{2+} release channel. Mol Cell Biochem 1992;114:119–123. [PubMed: 1334225]

28. McGarry SJ, Williams AJ. Activation of the sheep cardiac sarcoplasmic reticulum Ca^{2+}-release channel by analogues of sulmazole. Br J Pharmacol 1994;111:1212–1220. [PubMed: 8032608]
29. Radermacher M, Rao V, Grassucci R, Frank J, Timerman AP, Fleischer S, Wagenknecht T. Cryo-electron microscopy and three-dimensional reconstruction of the calcium release channel/ryanodine receptor from skeletal muscle. J Cell Biol 1994;127:411–423. [PubMed: 7929585]
30. Sharma MR, Penczek P, Grassucci R, Xin HB, Fleischer S, Wagenknecht T. Cryoelectron microscopy and image analysis of the cardiac ryanodine receptor. J Biol Chem 1998;273:18429–18434. [PubMed: 9660811]
31. Sharma MR, Jeyakumar LH, Fleischer S, Wagenknecht T. Three-dimensional structure of ryanodine receptor isoform three in two conformational states as visualized by cryo-electron microscopy. J Biol Chem 2000;275:9485–9491. [PubMed: 10734096]
32. Serysheva II, Orlova EV, Chiu W, Sherman MB, Hamilton SL, van Heel M. Electron cryomicroscopy and angular reconstitution used to visualize the skeletal muscle calcium release channel. Nat Struct Biol 1995;2:18–24. [PubMed: 7719847]
33. Wagenknecht T, Frank J, Boublik M, Nurse K, Ofengand J. Direct localization of the tRNA--anticodon interaction site on the Escherichia coli 30 S ribosomal subunit by electron microscopy and computerized image averaging. J Mol Biol 1988;203:753–760. [PubMed: 3062179]
34. Frank, J. Multivariate data analysis and classification of images. In: Frank, J., editor. Three-Dimensional Electron Microscopy of Macromolecular Assemblies. Oxford University Press; New York: 2006. p. 145-192.
35. Orlova EV, Serysheva II, van Heel M, Hamilton SL, Chiu W. Two structural configurations of the skeletal muscle calcium release channel. Nat Struct Biol 1996;3:547–552. [PubMed: 8646541]
36. Serysheva II, Schatz M, van Heel M, Chiu W, Hamilton SL. Structure of the skeletal muscle calcium release channel activated with Ca^{2+} and AMP-PCP. Biophys J 1999;77:1936–1944. [PubMed: 10512814]
37. Agrawal RK, Penczek P, Grassucci RA, Frank J. Visualization of elongation factor G on the Escherichia coli 70S ribosome: the mechanism of translocation. Proc Natl Acad Sci U S A 1998;95:6134–6138. [PubMed: 9600930]
38. Liu Z, Zhang J, Wang RW, Chen SRW, Wagenknecht T. Location of divergent region 2 on the three-dimensional structure of cardiac muscle ryanodine receptor/calcium release channel. J Mol Biol 2004;338:533–545. [PubMed: 15081811]
39. Meng X, Xiao B, Cai S, Huang X, Li F, Bolstad J, Trujillo R, Airey J, Chen SRW, Wagenknecht T, Liu Z. Three-dimensional localization of serine 2808, a phosphorylation site in cardiac ryanodine receptor. J Biol Chem 2007;282:25929–25939. [PubMed: 17606610]
40. Liu Z, Wang RW, Zhang J, Chen SRW, Wagenknecht T. Localization of a disease-associated mutation site in the three-dimensional structure of the cardiac muscle ryanodine receptor. J Biol Chem 2005;280:37941–37947. [PubMed: 16157601]
41. Perez CF, Mukherjee S, Allen PD. Amino acids 1-1,680 of ryanodine receptor type 1 hold critical determinants of skeletal type for excitation-contraction coupling. Role of divergence domain D2. J Biol Chem 2003;278:39644–39652. [PubMed: 12900411]
42. Wang R, Chen W, Cai S, Zhang J, Bolstad J, Wagenknecht T, Liu Z, Chen SRW. Localization of an NH_2-terminal disease-causing mutation hotspot to the “clamp” region in the three-dimensional structure of the cardiac ryanodine receptor. J Biol Chem 2007;282:17785–17793. [PubMed: 17452324]
43. McCarty TV, Quane KA, Lynch PJ. Ryanodine receptor mutations in malignant hyperthermia and central core disease. Hum Mutat 2000;15:410–417. [PubMed: 10790202]
44. Ikemoto N, Yamamoto T. Regulation of calcium release by interdomain interaction within ryanodine receptors. Front Biosci 2002;7:d671–d683. [PubMed: 11861212]
45. Zhou Q, Wang QL, Meng X, Shu Y, Jiang T, Wagenknecht T, Yin CC, Sui SF, Liu Z. Structural and Functional Characterization of Ryanodine Receptor-Natrin Toxin Interaction. Biophys J 2008;95:4289–4299. [PubMed: 18658224]
46. Brillantes AB, Ondrias K, Scott A, Kobrinsky E, Ondriasova E, Moschella MC, Jayaraman T, Landers M, Ehrlich BE, Marks AR. Stabilization of calcium release channel (ryanodine receptor) function by FK506-binding protein. Cell 1994;77:513–523. [PubMed: 7514503]

47. Gaburjakova M, Gaburjakova J, Reiken S, Huang F, Marx SO, Rosemblit N, Marks AR. FKBP12 binding modulates ryanodine receptor channel gating. J Biol Chem 2001;276:16931–16935. [PubMed: 11279144]
48. Samsó M, Shen X, Allen PD. Structural characterization of the RyR1-FKBP12 interaction. J Mol Biol 2006;356:917–927. [PubMed: 16405911]
49. Serysheva II, Hamilton SL, Chiu W, Ludtke SJ. Structure of Ca^{2+} release channel at 14 Å resolution. J Mol Biol 2005;345:427–431. [PubMed: 15581887]
50. Baker ML, Serysheva II, Sencer S, Wu Y, Ludtke SJ, Jiang W, Hamilton SL, Chiu W. Proc Natl Acad Sci U S A 2002;99:12155–12160. [PubMed: 12218169]
51. Chu A, Dixon MC, Saito A, Seiler S, Fleischer S. Isolation of sarcoplasmic reticulum fractions referable to longitudinal tubules and junctional terminal cisternae from rabbit skeletal muscle. Methods Enzymol 1988;157:36–46. [PubMed: 2976466]
52. Inui M, Saito A, Fleischer S. Purification of the ryanodine receptor and identity with feet structures of junctional terminal cisternae of sarcoplasmic reticulum from fast skeletal muscle. J Biol Chem 1987;262:1740–1747. [PubMed: 3805051]
53. Lai FA, Erickson HP, Rousseau E, Liu QY, Meissner G. Purification and reconstitution of the calcium release channel from skeletal muscle. Nature 1988;331:315–319. [PubMed: 2448641]
54. Yin CC, Lai FA. Intrinsic lattice formation by the ryanodine receptor calcium-release channel. Nat Cell Biol 2000;2:669–671. [PubMed: 10980710]
55. Fabiato A, Fabiato F. Calculator programs for computing the composition of the solutions containing multiple metals and ligands used for experiments in skinned muscle cells. J Physiol (Paris) 1979;75:463–505. [PubMed: 533865]
56. Favero TG, Zable AC, Abramson JJ. Hydrogen peroxide stimulates the Ca^{2+} release channel from skeletal muscle sarcoplasmic reticulum. J Biol Chem 1995;270:25557–25563. [PubMed: 7592726]
57. Dulhunty AF, Laver DR, Gallant EM, Casarotto MG, Pace SM, Curtis S. Activation and inhibition of skeletal RyR channels by a part of the skeletal DHPR II-III loop: effects of DHPR Ser687 and FKBP12. Biophys J 1999;77:189–203. [PubMed: 10388749]
58. Tanna B, Welch W, Ruest L, Sutko JL, Williams AJ. The interaction of an impermeant cation with the sheep cardiac RyR channel alters ryanoid association. Mol Pharmacol 2006;69:1990–1997. [PubMed: 16540598]
59. Miller C. Open-state substructure of single chloride channels from Torpedo electroplax. Philos Trans R Soc Lond B Biol Sci 1982;299:401–411. [PubMed: 6130538]
60. Frank J, Radermacher M, Penczek P, Zhu J, Li YH, Ladjadj M, Leith A. SPIDER and WEB: processing and visualization of images in 3D electron microscopy and related fields. J Struct Biol 1996;116:190–199. [PubMed: 8742743]
61. Frank, J. Computational correction of the contrast transfer function. In: Frank, J., editor. Three-Dimensional Electron Microscopy of Macromolecular Assemblies. Oxford University Press; New York: 2006. p. 58-62.
62. Liu Z, Zhang J, Sharma MR, Li P, Chen SRW, Wagenknecht T. Three-dimensional reconstruction of the recombinant type 3 ryanodine receptor and localization of its amino terminus. Proc Natl Acad Sci U S A 2001;98:6104–6109. [PubMed: 11353864]
63. Malhotra A, Penczek P, Agrawal RK, Gabashvili IS, Grassucci RA, Jünemann R, Burkhardt N, Nierhaus KH, Frank J. Escherichia coli 70 S ribosome at 15 Å resolution by cryo-electron microscopy: localization of fMet-tRNAfMet and fitting of L1 protein. J Mol Biol 1998;280:103–116. [PubMed: 9653034]

Abbreviations

CLIC
: Chloride intracellular channel

RyR
: ryanodine receptor

SR sarcoplasmic reticulum

2D two-dimensional

3D three-dimensional

Po open probability

To mean open time

Tc mean closed time

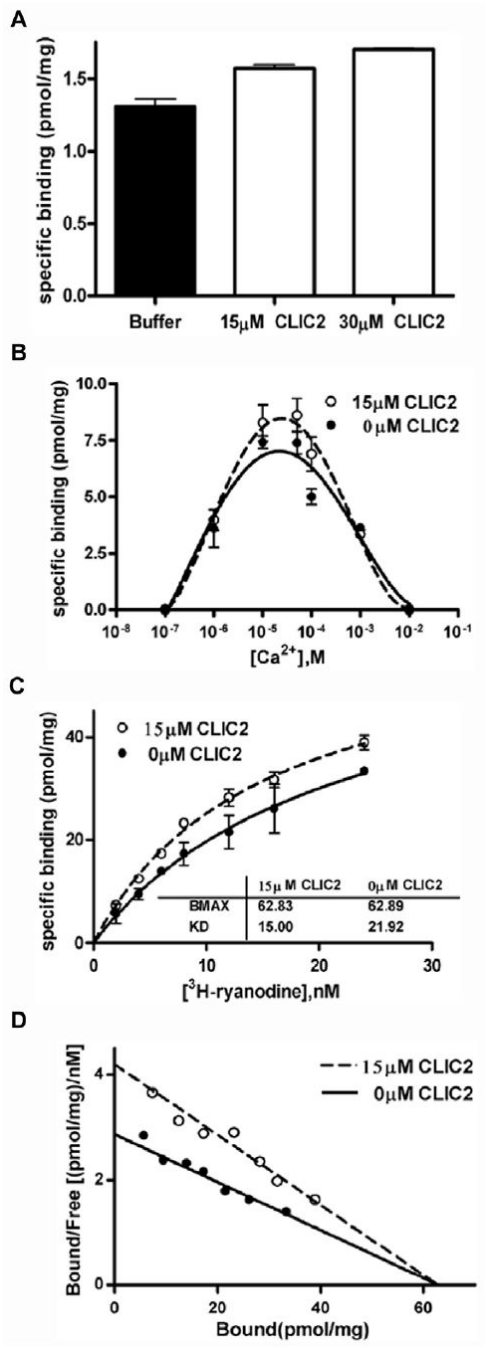

Figure 1. Effects of CLIC2 on [^{3}H]-ryanodine binding to skeletal heavy SR and purified RyR1

(A) CLIC2 increases [^{3}H]-ryanodine binding to skeletal heavy SR. Equilibrium binding experiments were performed in the absence or presence of CLIC2. The binding buffer contained 2 nM [^{3}H]-ryanodine and 10 μM Ca^{2+}. CLIC2 increased [^{3}H]-ryanodine binding to skeletal heavy SR from 1.31±0.1 pmol/ml (buffer, n=6) to 1.57±0.03 pmol/ml (15 μM CLIC2, n=6), and to 1.7±0.01 pmol/ml (30 μM CLIC2, n=6).

(B) CLIC2 increases [^{3}H]-ryanodine binding to purified RyR1. Equilibrium [^{3}H]-ryanodine binding experiments were carried out in binding buffer containing 2 nM [^{3}H]-ryanodine and various concentrations of Ca^{2+}, in the absence or presence of 15 μM CLIC2. [Ca^{2+}] was maintained, in a range between 0.1 μM and 10 mM, by a combination of EGTA and $CaCl_2$.

Free Ca^{2+} concentrations were calculated using the computer program of Fabiato and Fabiato.[51] Data points shown are the mean ± S.E.M. from three separate experiments.
(C) and (D) Equilibrium saturation assay of [^{3}H]-ryanodine binding to purified RyR1. Experiments were carried out in binding buffer containing 10 μM Ca^{2+}, and various concentrations of [^{3}H]-ryanodine (from 1 nM to 24 nM), in the absence or presence of 15 μM CLIC2, as described in the "Materials and methods". Panel C shows the saturation curves for [^{3}H]-ryanodine binding to purified RyR1. Inset are the best-fit values of B_{max} and K_d. Panel D shows the Scatchard analysis of panel C. Data points shown are the mean ± S.E.M., from three separate experiments.

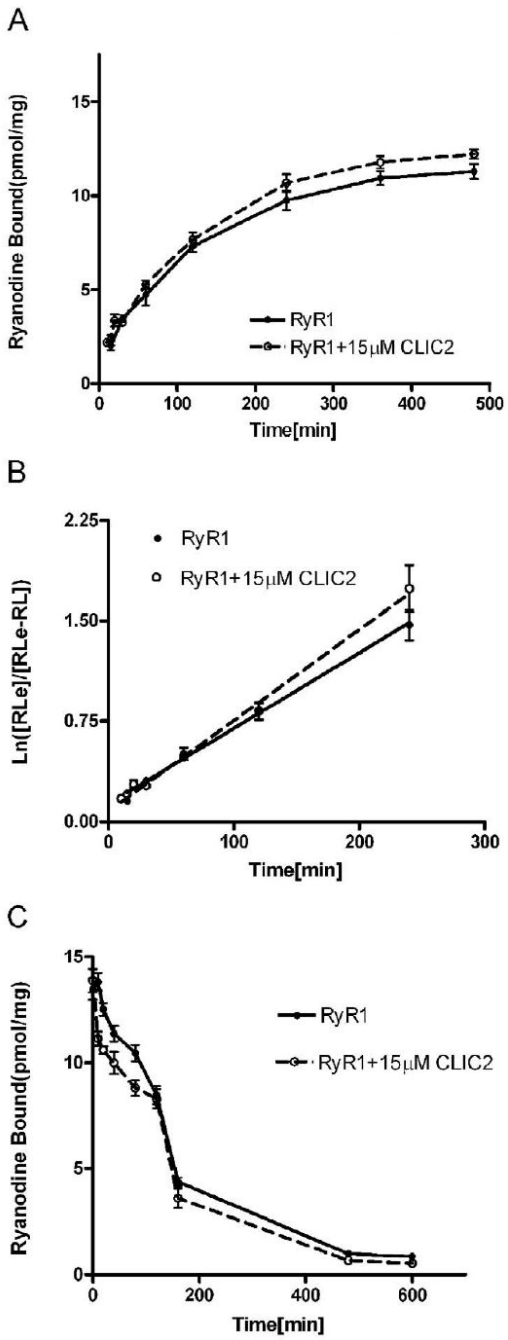

Figure 2. The effect of CLIC2 on binding kinetics of [^{3}H]-ryanodine to RyR1

(A) Time course of association of [^{3}H]-ryanodine to RyR1. The data shown are the average of six experiments.

(B) Linear transformation of A. This graph depicts the linear transformation of time-dependent association, where RL_e represents the amount of [^{3}H]-ryanodine bound at equilibrium, and *RL* represents the amount bound at any given time.

(C) Time course of dissociation of [^{3}H]-ryanodine from RyR1. The data shown are the average of five experiments.

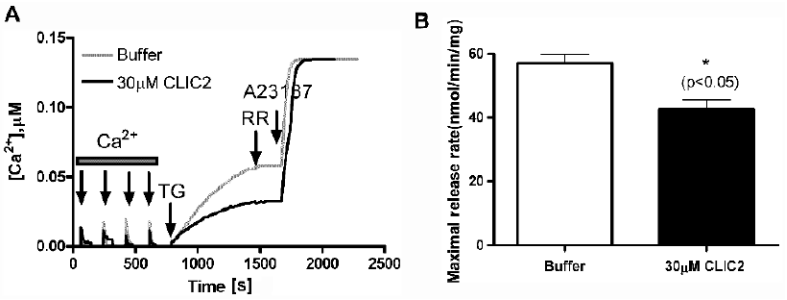

Figure 3. Effects of CLIC2 on Ca^{2+} efflux from skeletal SR vesicles

(A) Representative traces of extra vesicular [Ca^{2+}] variations measured with Antipyrylazo III as a Ca^{2+} indicator. These traces depict the process of Ca^{2+} uptake by Ca^{2+}-ATPase/pump after 4 applications of 7.5 μM CaCl2, Ca^{2+} efflux through RyR1 in presence of Thapsigargin, and total Ca^{2+} release from skeletal heavy SR vesicles at the end evoked by A23187. Experiments were divided into two groups, buffer (black) and 30 μM CLIC2 (gray), respectively. Arrows indicate the time points at which each reagent was added.

(B) Histogram of the maximal Ca^{2+} efflux rate from skeletal heavy SR vesicles. The asterisk denotes that the values are significantly different between the two groups, as assessed by *t*-test ($p<0.05$).

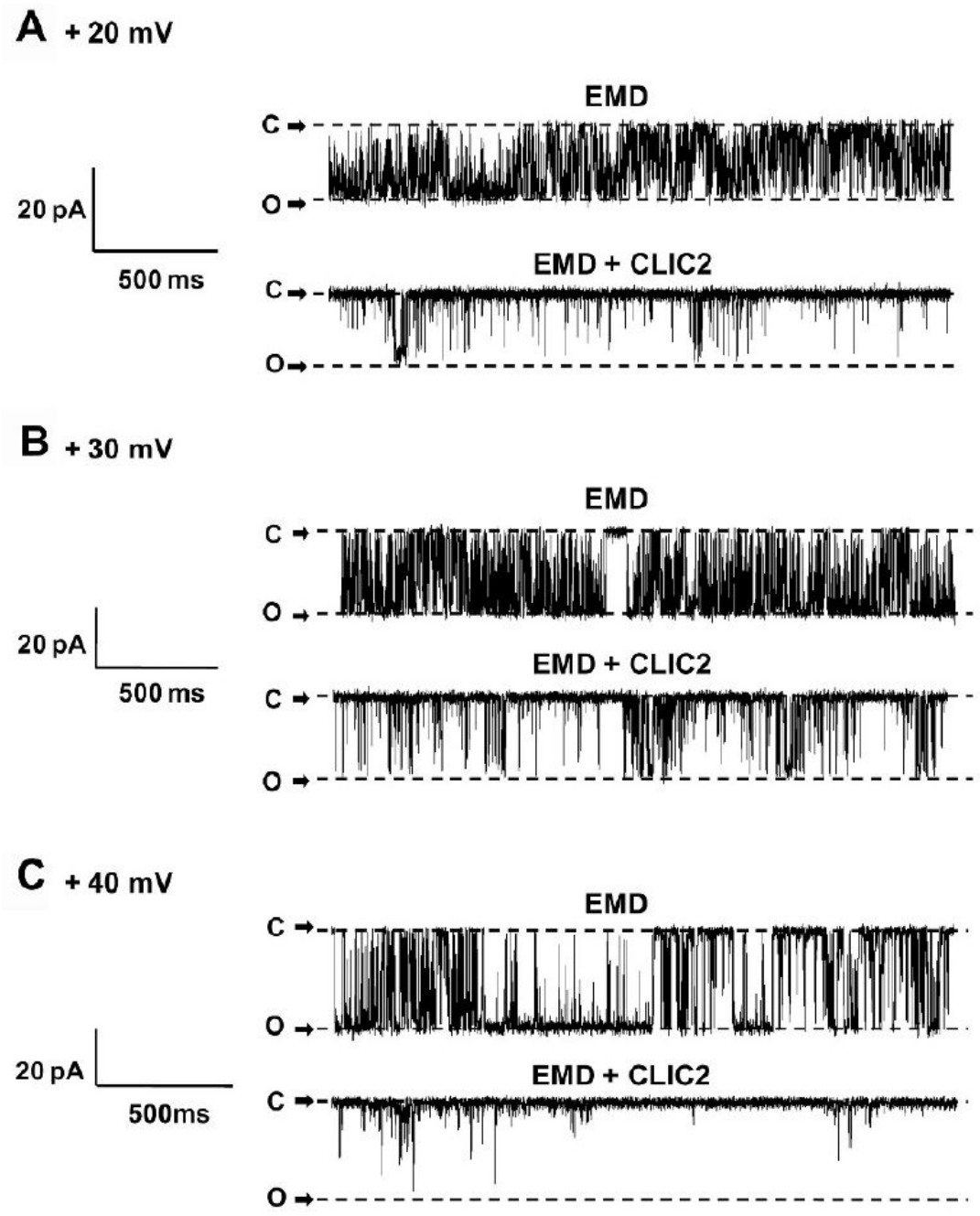

Figure 4. Single channel activity of purified RyR1 in presence of CLIC2

Depicted are representative single channel recordings (current flow *vs*. time) under EMD 41000 stimulation, with or without the addition of 7 μM CLIC2 at 3 different holding potentials: (A) +20 mV, (B) +30 mV, and (C) +40 mV. Both substances were applied to the cytosolic (*cis*) side of the channels. Closing and opening levels are indicated by an arrow and the letter 'C' or 'O', respectively. The traces were taken from data filtered at 1 kHz.

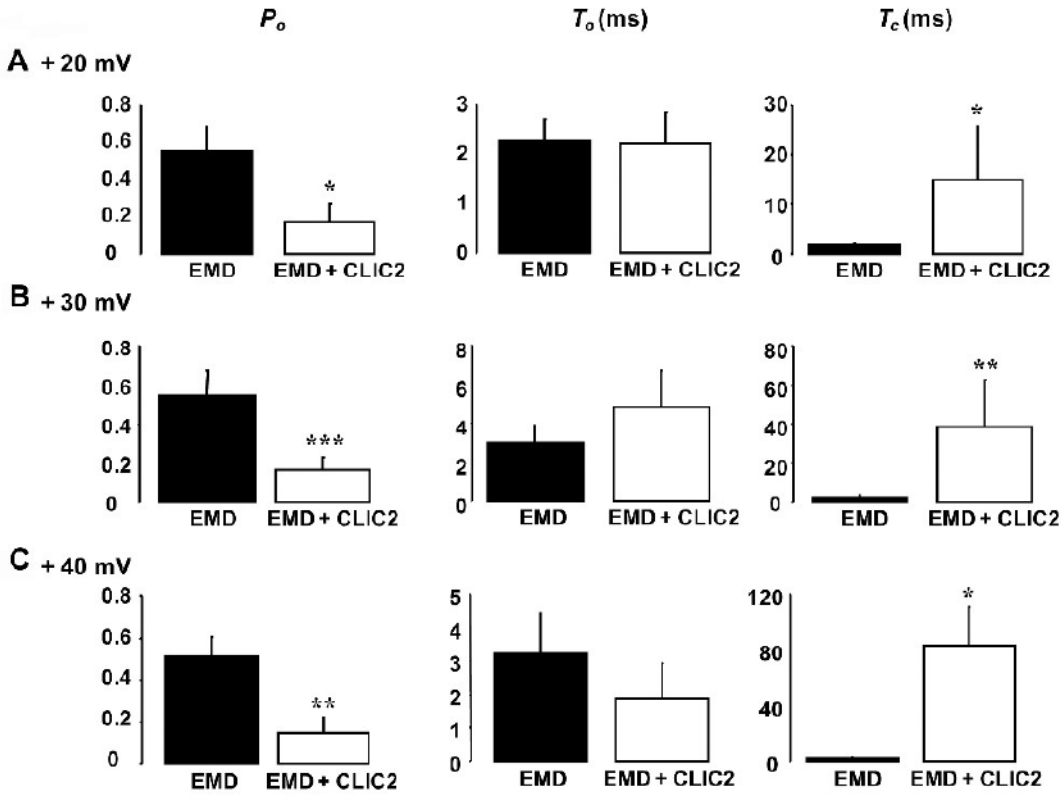

Figure 5. CLIC2 modifies gating parameters of the skeletal RyR1 channel

The analysis of three parameters is summarized in the histograms: mean open probability (P_O), mean open time (T_O), and mean close time (T_C). Comparisons of data that showed a significant difference from the value with EMD alone (black bars) have been marked with asterisks as follows: * $p \leq 0.05$, ** $p \leq 0.02$, *** $p \leq 0.01$. White bars represent parameters following the addition of CLIC2. The data were taken from 6 to 8 single channel experiments for +20 mV (A), 5 to 6 for +30 mV (B), and 6 to 11 for +40 mV (C).

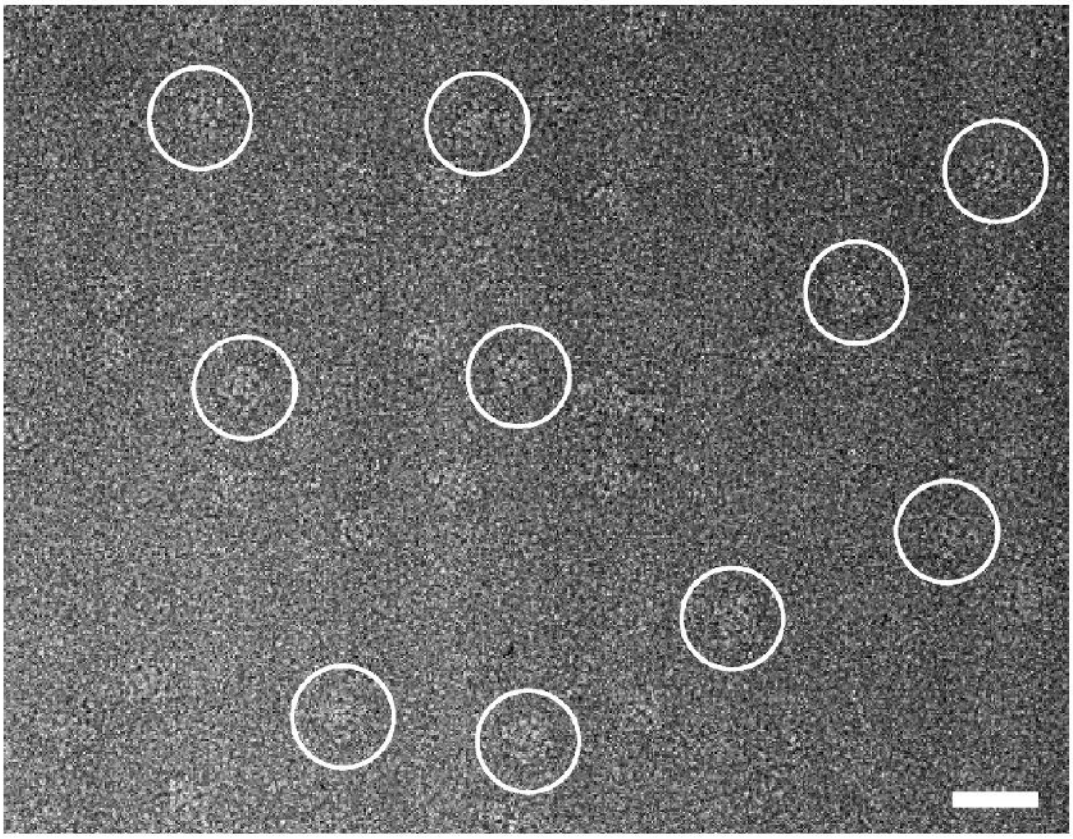

Figure 6. Cryo-electron microscopy of RyR1+CLIC2 complexes

Portion of cryo-EM micrograph of RyR1+CLIC2 complexes, with the protein particles embedded in a thin layer of vitreous ice. The tetrameric structure of RyR1 is well preserved as indicated by the characteristic square appearance, which represents the images of the particles lying with their 4-fold symmetry axes oriented perpendicular to the carbon support film. Several individual particles are marked with white circles. Scale bar = 500Å.

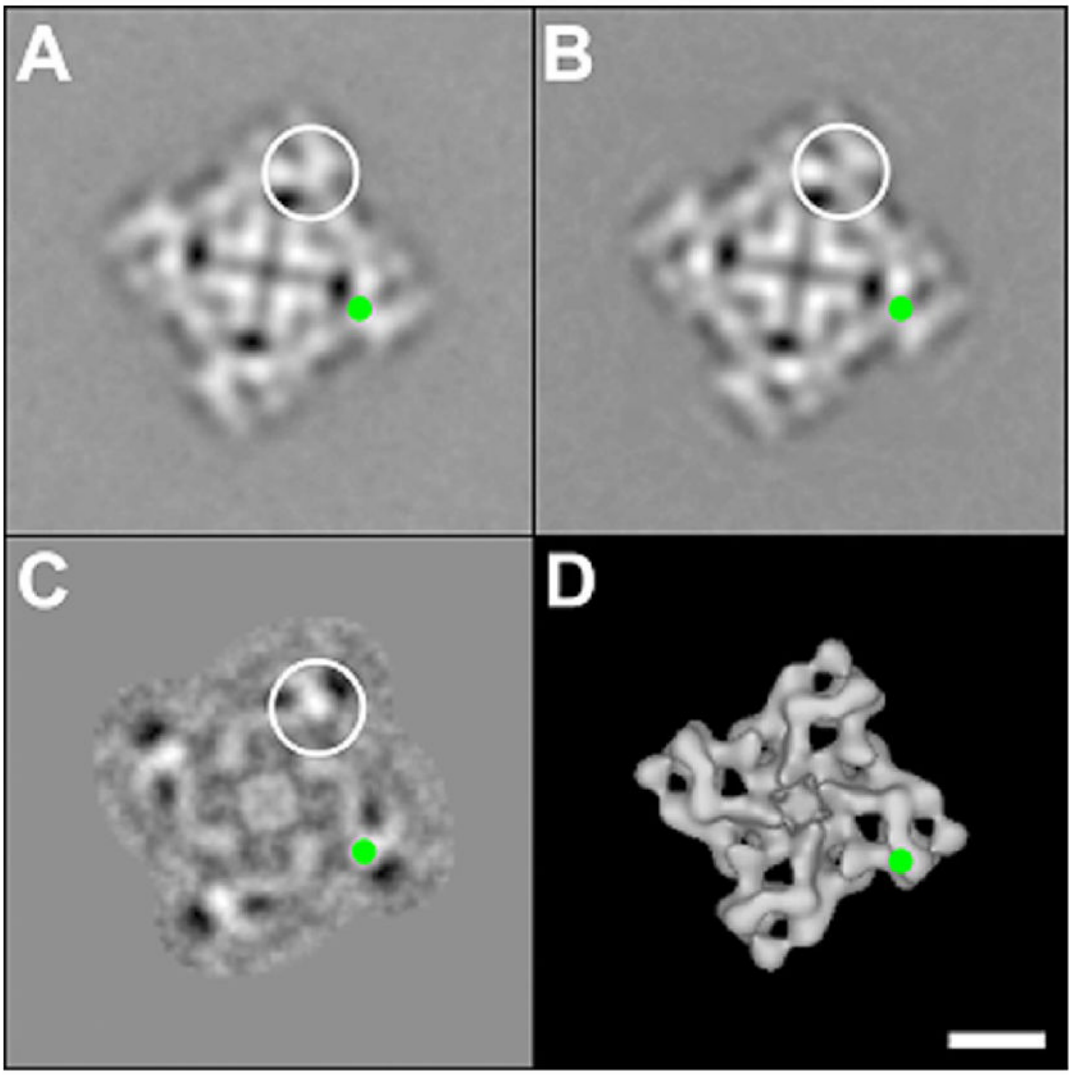

Figure 7. Two-dimensional averages of RyR1 and the RyR1+CLIC2 complex

(A) 2D average of the RyR1+CLIC2 complex (n = 297 particle images) in 'top' view; (B) Top view of the 2D average of RyR1 control (n = 317 particle images); (C) Difference map obtained by subtracting B from A. The top view represents the projection of the channel as seen from the cytoplasmic side, as shown in the cartoon in (D). The largest differences shown in (C), corresponding to the four additional masses contributed by binding of CLIC2, are seen as bright white areas, one of which is circled. The corresponding location of the major difference in (C) has been also highlighted with green dots in (A), (B), and (D). Scale bar = 100Å.

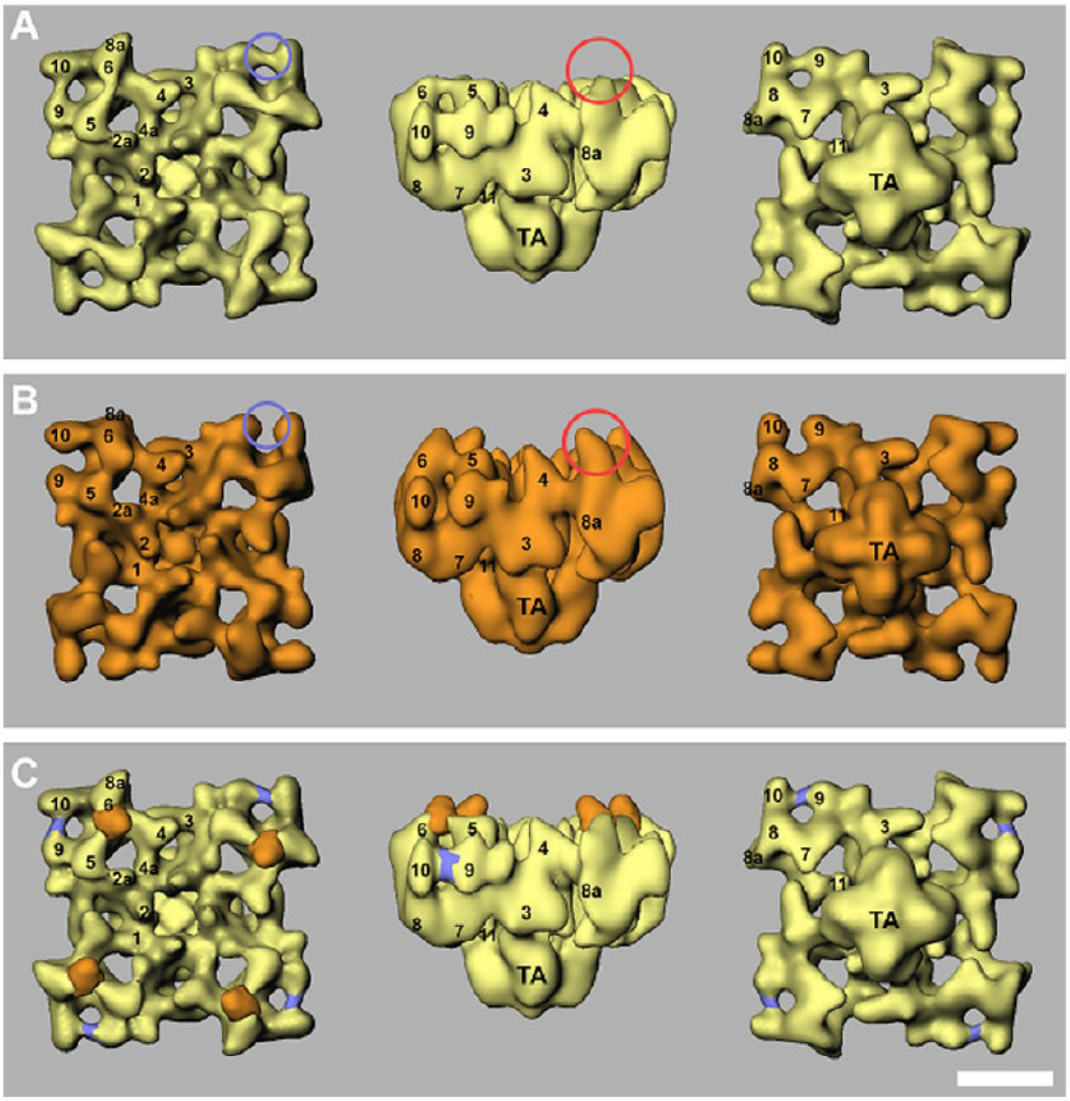

Figure 8. Three-dimensional surface representations of RyR1 and the RyR1+CLIC2 complex, and three-dimensional difference map

The 3D reconstruction of RyR1 is shown in yellow (panel A) and the RyR1+CLIC2 complex (panel B) is shown in orange. In panel C, the difference map (RyR1+CLIC2 minus RyR1) shown in orange is superimposed on the 3D reconstruction of RyR1 alone (yellow), another minor negative difference (RyR1 minus RyR1+CLIC2) shown in blue-violet, is also superimposed. The 3D reconstructions are shown in three views: left, top view from the cytoplasmic surface, which in situ would face the transverse tubule; middle, side view; right, bottom view showing the surface that would face the SR lumen. The numerals 1-11 on the cytoplasmic assembly indicate the distinguishable domains, according to our earlier nomenclature.[29] Scale bar = 100Å.

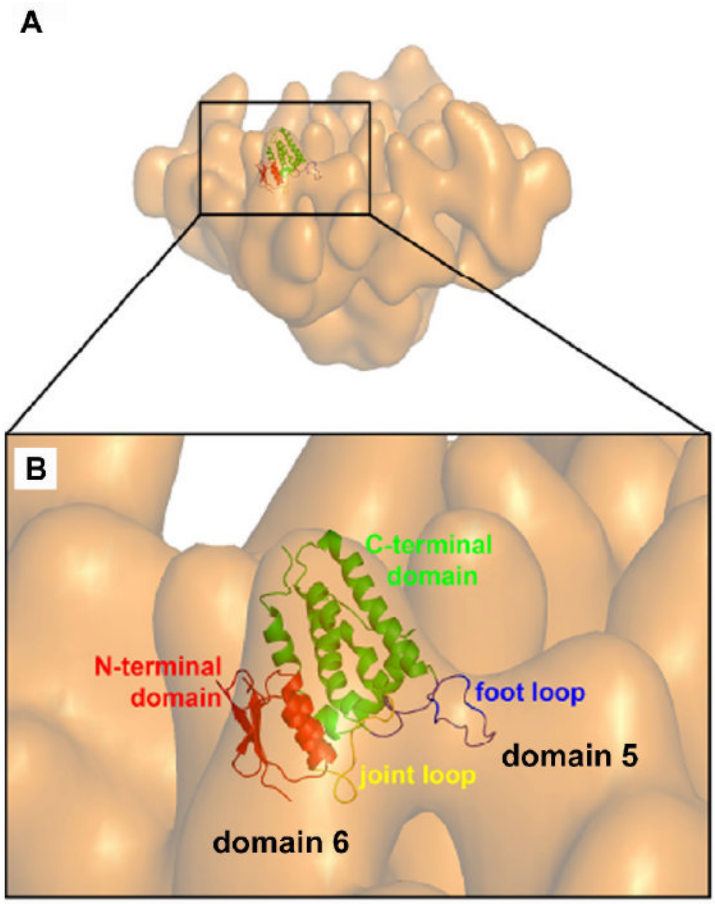

Figure 9. Docking of the X-ray crystal structure of CLIC2 into the cryo-EM density map of the RyR1+CLIC2 complex

The atomic coordinates of the CLIC2 (PDB code: 2PER) were manually fitted into our cryo-EM density map of RyR1+CLIC2 complex, using the program O. (A) A tilted view of the RyR1+ CLIC2 complex, with one CLIC2 molecule docked in the binding site of one subunit in the RyR1 homotetramer. (B) A zoomed view of the clamp region from (A), showing that CLIC2 binds to domains 5 and 6 of RyR1. Domain rendering of CLIC2 molecule: N-terminal domain (amino acid residues 11-94), red; joint loop (residues 95-106), yellow; C-terminal domain (residues 107-152 and 179-246), green; and foot loop, (residues 153-178), blue.

Table 1

The observed kinetics data for untreated RyR1 and RyR1 treated with 15 μM CLIC2

The k_{obs} was determined from linear transformation of the data shown in Figure 2A, k_{-1} was calculated according to $k_{-1} = \ln 2/t_{1/2}$ from the data shown in Figure 2C, where $t_{1/2}$ is the half dissociation time. $k_{+1} = (k_{obs} - k_{-1})/[L]$, where [L] is the total ligand concentration.

Treatment	k_{obs}	k_{-1}	k_{+1}	$K_d(k_{-1}/k_{+1})$
	min^{-1}	min^{-1}	$min^{-1}nM^{-1}$	nM
control	0.005642±0.00068 (n=6)	0.004959±0.00033 (n=5)	0.0003415	14.54
15 μM CLIC2	0.006791±0.00082 (n=6)	0.004934±0.00065 (n=5)	0.0009285	5.311